Licentiate Thesis

Developing Computational Methods for Moored Floating Wave Energy Devices

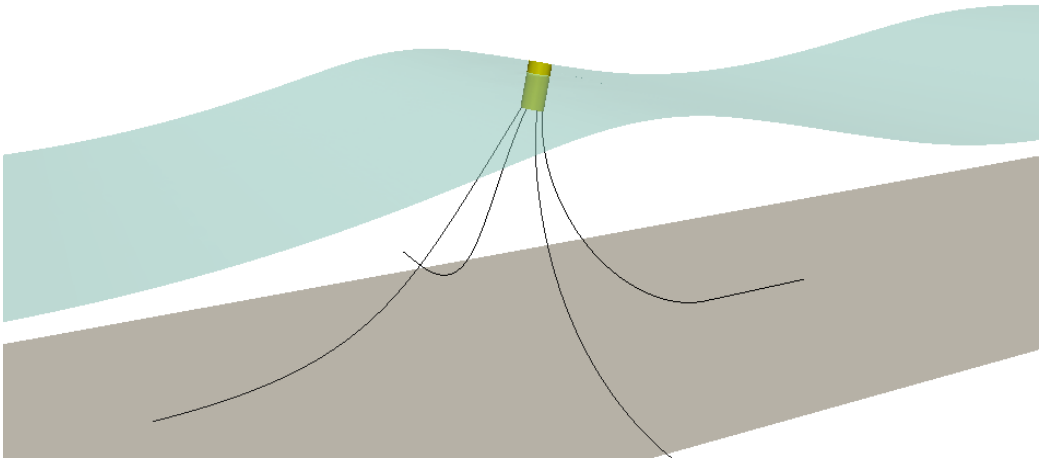

JOHANNES PALM

Department of Shipping and Marine Technology
CHALMERS UNIVERSITY OF TECHNOLOGY
Göteborg, Sweden 2014

Developing Computational Methods for Moored Floating Wave Energy Converters

JOHANNES PALM

Report no 14:151
ISSN 1652-9189

Department of Shipping and Marine Technology
Chalmers University of Technology
SE-412 96 Göteborg
Sweden
Telephone + 46 (0)31-772 1000

Printed by Chalmers Reproservice
Göteborg, Sweden 2014

ACKNOWLEDGEMENT

I gratefully acknowledge the support from Västra Götalandsregionen for their support of the Ocean Energy Centre (OEC) that has made this project possible. The OEC has provided a close connection between myself, my supervisors and the industrial partners of the OEC and I hope for continued discussions in the years to come.

Much of the results in this thesis have been produced in close collaboration with Guilherme Moura Paredes from the University of Porto, Portugal. I am very glad for the opportunity to work so closely with him during my first two years of research. I especially enjoyed the time I spent in Portugal with Guilherme doing experimental work on mooring configurations.

My deepest gratitude to Claes Eskilsson and Lars Bergdahl, for without your knowledge and encouragement this thesis would not have been. Also, I would like to thank my examiner Rickard Bensow and my colleagues at the group of hydrodynamics for all your help, and for humouring me whenever I torment you with odd and detailed questions about a particular problem.

Finally, my love and thanks goes to my wife, mother, family and friends for helping me view my work from the right perspective.

Abstract

Floating point absorbers are a common class of wave-power devices typically designed to move with large amplitude in energetic waves. This stands in sharp contrast to traditional marine design, where the wave-excited motions of the structure are preferably kept to a minimum. Large motions in relatively shallow water increase the risk of slack in the mooring cables, which in turn causes snap loads of large amplitude that might affect the design loads of the moorings. Thus, a high level of non-linearity is introduced in both the mooring force response and the device motion in waves. Furthermore, there is a strong coupling between the two problems, so they cannot be solved independently. These requirements are not fully covered by conventional methods of marine design, implying a need for further development of methods.

This thesis describes the development of MooDy, a modular, Finite Element (FE) code for mooring cable dynamics. The spatial discretisation is realised by a modified version of the Local Discontinuous Galerkin method with high-order polynomial basis functions. Further, a coupled computational method for the dynamics of moored, floating wave energy converters (WECs) is presented, and applied to two generic WECs in regular waves. MooDy interacts with a separate solver for the hydrodynamic problem through an Automated Program Interface (API) communicating fair-lead position and tension force at each time step. The API is used to communicate with both a standard, linear potential flow solver and a Reynolds Averaged Navier Stokes (RANS) solver. The RANS simulations are done with the OpenFOAM platform, and the free surface is captured using the Volume of Fluid (VoF) method. This approach has the potential to encompass effects from viscous forces, instantaneous water level, green water and breaking, non-linear waves; all the while taking non-linear mooring restraint into account. Thus, the suggested method strives for completeness, although it comes at a high computational cost.

Results from MooDy exhibit the theoretically predicted exponential convergence for smooth solutions, and compare well with experimental data. The model supports propagating tension-waves with very little numerical damping; a feature that is not available in commercial codes. However, some numerical fluctuations in the tension force are noted, due to the numerical implementation of the sea-bed interaction and the loss of structural stiffness in the slacking of the cable. The computational cost of the coupled RANS-Mooring solver is very high, and preliminary results show large deviations from the predictions by linear theory for the resonance region of a generic WEC. As the body moves with large amplitude, the deviation is the combined effect of fully non-linear exciting wave force, viscous forces, non-linear mooring restraint and numerical damping due to an under-resolved boundary layer around the structure. Work with the quantification of the individual importance of these effects is ongoing.

CONTENTS

1

Introduction

1.1 Background and Motivation

There is a large variety of techniques for wave energy extraction, ranging from large ($D \sim 100\,\mathrm{m}$) floating platforms to small ($D \sim 5\,\mathrm{m}$) point absorbing bodies. Each concept has individual challenges, but common for all is a need of reliable design and evaluation methods. The well-proven methods used in naval architecture and the off-shore industry are used when applicable, but the requirements of many Wave Energy Converters (WECs) are very different. This is highlighted by the properties of a common class of WECs named floating point absorbers.

A point-absorbing WEC is a buoy designed to move with large amplitude in or near its resonance frequency. It is small in relation to the wavelength of the mean waves at the deployment site, and is commonly placed in shallow to intermediate water depths. Large displacements in shallow water puts very tough requirements on the moorings as high compliance is needed to allow the structure to move in operational conditions. At the same time, the moorings must be reliable, durable, and preferably have a minimal footprint. Since point absorbing WECs will be installed in arrays (or parks), a smaller footprint gives a denser array and therefore yields a more efficient extraction of the wave energy for the park in total. For these reasons accurate computational models of mooring cable dynamics are important tools in the mooring design process of floating WECs.

Because of the moderate buoy-size, the increased stiffness and induced damping due to the presence of the moorings are not negligible in comparison with the hydrodynamic forces. Models for the motion of the moored device should therefore take the coupling between restraining mooring forces and time-varying hydrodynamic loads into account. Moreover, to estimate the amount of energy produced by a device, there is a need for high accuracy in the resonance region

of the body where the bulk of the wave energy is absorbed. Resonance is traditionally studied to accommodate for maximum loads only, allowing for a conservative calculation approach. As this over-estimates the motion and thereby also the energy production, it is clearly not suitable for floating WECs. For survival situations such as storms, the non-linearities in the coupled problem of mooring dynamics and wave-excited motion become larger and the methods need to be refined accordingly if a cost-effective design is to be achieved.

The maximum time step size of explicit time-integration methods for cable models is severely limited by the high speed of sound in the cable. Therefore implicit methods that allow larger time steps are commonly used. However, an increasing level of numerical diffusion is imposed on the solution as the time-step size is increased. To resolve a shock-wave in the tension force - arising from cable slack, sudden motions of the fair-lead or ground interaction - a model with very low numerical diffusion is needed. To model such shocks accurately using commercial mooring codes is therefore very difficult. There are few documented model-scale experiments where the sampling frequency is high enough to account for these fast propagating loads and therefore their effect in WEC applications is not yet fully known.

1.2 Content description

The thesis presents a coupled approach for modelling the motion of moored, floating wave energy converters, including a new model for mooring cable dynamics. Chapter 2 describes the governing equations of cable dynamics and the formulation of the MooDy software. Three papers are appended to the thesis, summarised in Chapter 3. Paper I describes the formulation, verification and validation of MooDy, and Paper II and III present two examples of MooDy's modular capability. In Paper II it is coupled to a linear time-domain solver for the WEC motion, while Paper III contains the proof of concept of a coupling to the `interDyMFoam` RANS-solver in OpenFOAM [25]. The thesis ends with a discussion of possible applications, benefits and drawbacks of the methods and a description of ongoing and future work.

1.3 Previous studies

As a metric for the commercial readiness of WEC developers and their technology, the concepts of Technology Readiness Levels (TRLs) [14] and Technology Performance Levels (TPLs) [31] have been proposed. Both scales are defined from level 1 to level 9, with 9 being the maximum. TRL is a measure of the commercial readiness of a concept while TPL scales more directly to the LCOE (Levelized Cost Of Energy) of the product. In [31], Weber assessed wave energy companies according to these two metrics, concluding that most developers tended to focus more on the readiness than on the performance of the technol-

ogy. He suggested that a more economically viable route to reach level 9 in both metrics could be achieved by shifting focus and instead have performance first in mind in the technology development. In assessing the performance of a device (i.e. the TPL), reliable and accurate computational methods are crucial. The following subsections present common practice for WEC design and state-of-the-art studies on the modelling of cable dynamics and hydrodynamics for WECs.

1.3.1 Hydrodynamic models

The most suitable choice of method for computing the motions of a moored, floating WEC in waves is naturally that which best matches the purpose of the computation. A good method for extreme loads under storm conditions is not necessarily appropriate for computing the fatigue loads in moderate waves, and vice versa. Linearised potential flow solvers in frequency domain is by far the most common tool available for estimating the motions of floating structures. When Cummins introduced the impulse-response-function approach in naval architecture [8], these methods were extended to the time domain by using a convolution integral for the memory term, and hydrodynamic coefficients derived from the radiation-diffraction problem of small displacements around the mean water level. The coefficients are commonly taken from numerical simulations in e.g. the potential flow code WAMIT [30], but they can be calculated analytically in cases of simple geometry; see e.g. [17] for a description of the Green's function problem around a cylinder. With chosen coefficients, the time history of the motion can be computed in the time or frequency domain. One of the most popular implementations in the time domain is the state-space model [33]. This has the benefit of allowing non-linear mooring load input, thus enabling proper coupling. If instead the mooring response is disregarded or linearised, a frequency domain solver can be utilised, resulting in a very high computational speed. Such a linearisation was suggested and outlined by Fitzgerald and Bergdahl [13].

All of these methods are however relatively fast, and are therefore widely used to compute the overall WEC response over sea-state time ranges (in the order of three hours). One of the more complete studies is found in [4], where a wave-to-wire model is used to estimate the performance of eight generic concepts at five European sites. Being based on the linearised free surface boundary condition, this does not take into account viscous effects, breaking waves or non-linear excitation forces, and the authors recognise the inaccuracy of the method in extreme waves and close to resonance.

Following the development of computer performance, the use of Computational Fluid Dynamics (CFD) has steadily increased in marine applications and is now common practice within naval architecture [19]. Although the use of CFD is still limited within wave energy, an increasing number of studies using RANS-simulations has been presented over the last few years. Bhinder et. al. [5] compared forces from a RANS-simulation with the first order Morison force, and

studied the viscous force contribution. In their case, the viscous force was found to be small, and few other studies on the viscous effects on WECs are available. Wave propagation and resulting wave forces on fixed surface-piercing and submerged structures were studied by Li and Lin [20]. They presented results for both regular and irregular waves, including a comparison with analytic and experimental results and also with other numerical methods. A method for free-floating bodies including fluid-structure interaction has been presented in [2], where a full sea-state with two floating, generic bodies was computed.

An example of work on floating WECs using RANS that include moorings can be found in [32], where the mooring system was approximated as a linear spring. Thus, the linearised, first-order representation of the mooring restraint on the device motion was used. A more complete model was presented in the pioneering work of Aliabadi et al. [3] that described a CFD simulation of a generic ship in large waves with over-topping waves, coupled with a dynamic mooring force calculation using FEM. The coupled method presented in this thesis is an extension of that approach.

1.3.2 Mooring cable studies

A slack mooring system - where the reaction from catenary chains is the main elastic component - is commonly used for mooring floating WECs. Fitzgerald evaluated and compared several mooring configurations [12], showing that the choice of mooring system significantly influences the device performance. He also evaluated the effect of the attachment point position on the floating body [13]. In his work, a financial perspective on moorings shows how an optimal array configuration can play a future key role in the economics of a wave energy site.

The damping effects of moorings and their importance for WEC design has been emphasised by Johanning et al. in e.g. [16], where the energy absorbed by the sea-bed in a slack mooring system is included. In studying the sea-bed interaction of the cable, Triantafyllou [29] has shown the importance of the Touch Down Point (TDP), where the mooring cable first touches the ground. He showed that a shock-wave appears when the speed of the TDP exceeds the transverse wave speed of the cable. This was later corroborated by Gobat and Grosenbaugh in [15], where an experimental study of a slack cable on one rigid and one porous sea-bed type was conducted. For some frequencies, the presence of the shock-wave was clearly seen in the measured tension force at the fairlead. These shocks were quickly dissipated through frictional losses between the cable and the ground.

1.3.3 Mooring modelling

The early mooring models used in the off-shore oil industry for semi-submersible platforms were commonly quasi-static [23]. This is indeed still a valid design method for the mooring loads for the hydro-carbon industry and for floating wind

power plants [9, 10]. In the late 1990s, Brown and Mavrakos [6] compared different cable models, focusing on the type of model and its performance in a number of test cases. They concluded that models in the time-domain agreed well across different implementations, while frequency-domain and quasi-static simulations showed large inaccuracies in the tension force for some test cases. In [28], Spak et al. presented an account of the developments in cable modelling, with emphasis on internal damping models for helical cables. Although their paper was not aimed at marine applications, they have included a compiled list of different formulations of cable dynamics, the basic assumptions and the authors working on each approach.

In [24], Montano et. al. described a mixed element method for cable dynamics. Here the tension force was handled as a discontinuous variable, and the position of the cable was continuous. Using implicit time stepping, the work focused on inextensible ($E = \infty$) cables, and the analogy to the implementation of incompressible fluid solvers was pointed out. The cable model was implemented with high-order polynomial basis functions, and was block-coupled to a linear solver for the rigid body motion in waves.

2

Cable dynamics

2.1 INTRODUCTION

This chapter describes the theoretical framework of the cable modelling software MooDy, its underlying assumptions and finite element formulation. The code is at present written in the Matlab code language, although a stand-alone version in C++ is under development. The content is to a large extent compiled from Paper I, where the full description of the original formulation can be found.

2.2 GOVERNING EQUATION

The main assumption of many dynamic cable models is that the effect of bending and torsional stiffness can be neglected. The equation of motion for the cable position $\mathbf{r} = (r_x, r_y, r_z)$ expressed along the curvilinear abscissa s of the unstretched, perfectly flexible cable, can be written as a coupled set of non-linear wave equations. Following [1, 24] the formulation for a linearly elastic cable material appears as

$$\frac{\partial^2 \mathbf{r}}{\partial t^2} = \frac{1}{\gamma_0}\frac{\partial}{\partial s}\left(\frac{T}{1+\varepsilon}\frac{\partial \mathbf{r}}{\partial s}\right) + \frac{\mathbf{f}}{\gamma_0}, \tag{2.1}$$

$$T = EA_0\varepsilon, \tag{2.2}$$

$$\varepsilon = \left|\frac{\partial \mathbf{r}}{\partial s}\right| - 1, \tag{2.3}$$

where γ_0 is the mass per meter cable, T represents the axial tension force, and ε is the cable tangential strain. The linear, axial stiffness of the cable is denoted by EA_0. All external forces are here represented as $\mathbf{f}$.

Table 2.1: Choice of characteristic values used for rendering the system non-dimensional. L denotes the unstretched length of the cable.

Label (Unit)	Value
L_c (m)	L
m_c (kg)	$L_c \gamma_0$
K_c (N)	EA_0
t_c (s)	$\sqrt{\frac{m_c L_c}{K_c}}$

2.2.1 Non-dimensional formulation

The cable equations are non-dimensionalised through characteristic values of length, mass, force, and time, all chosen from the physical quantities of the cable. The values of the characteristic scales are presented in table 2.1. In this chapter, all equations and variables are given in their non-dimensional form.

2.2.2 External forces

The total force from the environment acting on a cable segment is here subdivided into six terms, according to $\mathbf{f} = \mathbf{f}_1 + \mathbf{f}_2 + \mathbf{f}_3 + \mathbf{f}_4 + \mathbf{f}_5 + \mathbf{f}_6$.

$\mathbf{f}_1$: The sum of gravity and buoyancy

$\mathbf{f}_2$: Tangential added mass force

$\mathbf{f}_3$: Normal added mass force

$\mathbf{f}_4$: Tangential drag force

$\mathbf{f}_5$: Normal drag force

$\mathbf{f}_6$: Contact forces

To simplify expressions, we introduce the unit tangential vector $\mathbf{t}$ as

$$\mathbf{t} = \frac{\partial \mathbf{r}}{\partial s} \Big/ \left| \frac{\partial \mathbf{r}}{\partial s} \right| = \frac{\partial \mathbf{r}}{\partial s} \Big/ (1+\varepsilon) \ , \tag{2.4}$$

and the decomposition notations $\mathbf{x}_\mathrm{t} = (\mathbf{x} \cdot \mathbf{t})\,\mathbf{t}$ and $\mathbf{x}_\mathrm{n} = \mathbf{x} - \mathbf{x}_\mathrm{t}$ for the tangential and normal components of a vector $\mathbf{x}$. Thus the external force contributions of added

mass and drag forces according to the Morison assumption read

$$\mathbf{f}_1 = -\gamma_e \mathbf{g}, \tag{2.5}$$

$$\mathbf{f}_2 = A_0 \rho_w \left(C_{Mt} \mathbf{a}_{rel,t} + \mathbf{a}_{w,t} \right), \tag{2.6}$$

$$\mathbf{f}_3 = A_0 \rho_w \left(C_{Mn} \mathbf{a}_{rel,n} + \mathbf{a}_{w,n} \right), \tag{2.7}$$

$$\mathbf{f}_4 = \frac{1}{2} C_{Dt} \rho_w d \left| \mathbf{v}_{rel,t} \right| \mathbf{v}_{rel,t} \left(1 + \varepsilon \right), \tag{2.8}$$

$$\mathbf{f}_5 = \frac{1}{2} C_{Dn} \rho_w d \left| \mathbf{v}_{rel,n} \right| \mathbf{v}_{rel,n} \left(1 + \varepsilon \right), \tag{2.9}$$

where ρ_c and ρ_w are the cable and fluid densities, and

$$\gamma_e g = \left(\left(\rho_c - \rho_w \right) / \rho_c \right) \gamma_0 g, \tag{2.10}$$

is the effective weight per unit length of the submerged cable. Further d is the nominal cable diameter and A_0 is its cross-sectional area. The terms C_{Mt}, C_{Mn}, C_{Dt} and C_{Dn} denote the hydrodynamic coefficients of added mass and drag forces respectively. Forces $\mathbf{f}_2$ to $\mathbf{f}_5$ depend on the relative velocity and relative acceleration of the water with respect to the mooring cable, $\mathbf{v}_{rel}$ and $\mathbf{a}_{rel}$. These are given by

$$\mathbf{v}_{rel} = \mathbf{v}_w - \frac{\partial \mathbf{r}}{\partial t}, \tag{2.11}$$

$$\mathbf{a}_{rel} = \mathbf{a}_w - \frac{\partial^2 \mathbf{r}}{\partial t^2}, \tag{2.12}$$

where $\mathbf{v}_w$ and $\mathbf{a}_w$ are the velocity and acceleration of the fluid. The second terms in 2.6 and 2.7 only depend on the fluid acceleration, and represent the Froude-Krylov forces acting on the cable segment.

The contact force $\mathbf{f}_6$ is the force acting on the cable from the ground. The ground is modelled as a bi-linear spring and damper for the normal direction (following [26]) and with viscous friction along the tangential plane (following [21]). The ground response force is for a horizontal ground calculated according to eq. (2.13)-(2.16), where K is the Winkler module (Pa/m), $\xi \leq 0$ is the ratio of critical damping, μ is the coefficient of dynamic friction, and v_c is the cut-off speed of the viscous friction force.

$$f_{6z} = Kd \left(r_z - z_g \right) - 2\xi \sqrt{\gamma_0 K d} \max \left(\dot{r}_z, 0 \right) \tag{2.13}$$

$$\mathbf{v}_{xy} = \frac{(v_x, v_y)}{\max \left(v_c, |(v_x, v_y)| \right)} \tag{2.14}$$

$$\mathbf{f}_{6xy} = -\gamma_e g \mu \sin \left(\mathbf{v}_{xy} \frac{\pi}{2} \right) \tag{2.15}$$

$$\mathbf{f}_6 = (\mathbf{f}_{6xy}, f_{6z}) \tag{2.16}$$

2.3 DISCRETISATION

MooDy is based on the Local Discontinuous Galerkin Method (LDG). The cable domain Ω is discretised into N_{el} elemental domains $\Omega^e \in \left[s_l^e, s_u^e\right]$, where s_l^e and s_u^e are the upper and lower edges of the element.
Equation (2.1) is first rewritten as a first order equation system in space with the introduction of an auxiliary variable $\mathbf{q}$:

$$\frac{\partial^2 \mathbf{r}}{\partial t^2} = \frac{1}{\gamma_0}\frac{\partial}{\partial s}\left(\frac{T}{1+\varepsilon}\mathbf{q}\right) + \frac{\mathbf{f}}{\gamma_0}, \tag{2.17}$$

$$\mathbf{q} = \frac{\partial \mathbf{r}}{\partial s}, \tag{2.18}$$

$$\varepsilon = |\mathbf{q}| - 1. \tag{2.19}$$

Introducing the cable vector force $\mathbf{T}$ as

$$\mathbf{T} = EA_0\varepsilon\frac{\mathbf{q}}{1+\varepsilon} = T\mathbf{t}, \tag{2.20}$$

equation (2.17) can be condensed into

$$\frac{\partial^2 \mathbf{r}}{\partial t^2} = \frac{1}{\gamma_0}\frac{\partial \mathbf{T}}{\partial s} + \frac{\mathbf{f}}{\gamma_0}. \tag{2.21}$$

Within the e^{th} elemental region, the solution for an arbitrary function f is approximated by setting $f(s,t) \approx f_h^e(s,t) = \sum_{i=0}^{i=p} \phi_i(s)\tilde{f}_i^e(t)$. Here $\tilde{f}_i^e(t)$ are the local degrees of freedom of expansion coefficients, and ϕ_i are the expansion basis of order i.
Denoting the inner product by $(\cdot,\cdot)$, the Galerkin approximation of equations (2.18), (2.20) and (2.21) is obtained as

$$\left(\phi_k, \frac{\partial^2 \mathbf{r}_h}{\partial t^2}\right)_{\Omega^e} = \frac{1}{\gamma_0}\left(\phi_k, \frac{\partial \mathbf{T}_h}{\partial s}\right)_{\Omega^e} + \frac{1}{\gamma_0}\left(\phi_k, \mathbf{f}_h\right)_{\Omega^e}, \qquad \forall\, k, \tag{2.22}$$

$$\left(\phi_k, \mathbf{q}_h\right)_{\Omega^e} = \left(\phi_k, \frac{\partial \mathbf{r}_h}{\partial s}\right)_{\Omega^e}. \tag{2.23}$$

Integrating the terms involving derivatives of s by parts, exchanging the boundary flux terms with numerical fluxes, and integrating by parts once more yields

$$\left(\phi_k, \frac{\partial^2 \mathbf{r}_h}{\partial t^2}\right)_{\Omega^e} = \frac{1}{\gamma_0}\left(\phi_k, \frac{\partial \mathbf{T}_h}{\partial s}\right)_{\Omega^e} + \frac{1}{\gamma_0}\left[\phi_k(\widehat{\mathbf{T}_h^e} - \mathbf{T}_h^e)\right]_{s_l^e}^{s_u^e} + \frac{1}{\gamma_0}\left(\phi_k, \mathbf{f}_h\right)_{\Omega^e}, \tag{2.24}$$

$$\left(\phi_k, \mathbf{q}_h\right)_{\Omega^e} = \left(\phi_k, \frac{\partial \mathbf{r}_h}{\partial s}\right)_{\Omega^e} + \left[\phi_k(\widehat{\mathbf{r}_h^e} - \mathbf{r}_h^e)\right]_{s_l^e}^{s_u^e}, \tag{2.25}$$

where numerical fluxes are denoted by $\widehat{\cdot}$. This is the Galerkin formulation for discontinuous FE, and the choice of numerical fluxes decides both the stability

and the computational stencil of the formulation. A modified version of the local discontinuous Galerkin (LDG) method developed by Cockburn and Shu [7] is used in this thesis:

$$\widehat{\mathbf{r}_h} = \{\mathbf{r}_h\} + \beta\,[\mathbf{r}_h]\,, \tag{2.26}$$

$$\widehat{\mathbf{T}_h} = \{\mathbf{T}_h\} - \beta\,[\mathbf{T}_h] + \frac{\eta_1}{h}\,[\mathbf{r}_h] + \eta_2 h\,[\mathbf{v}_h]\,. \tag{2.27}$$

Here η_1 and η_2 are constant mesh-independent parameters, h is the non-dimensional element size, $\beta \in [-1/2, 1/2]$ controls the level of up- and down-winding of the fluxes, and the trace $\{x\}$, and jump $[x]$ operators are defined as

$$\{x_h^e\}|_s = \frac{1}{2}\left(x_h^e|_{s_u^e} + x_h^{e+1}|_{s_l^{e+1}}\right) \quad \text{if} \quad s = s_u^e\,, \tag{2.28}$$

$$\{x_h^e\}|_s = \frac{1}{2}\left(x_h^e|_{s_l^e} + x_h^{e-1}|_{s_u^{e-1}}\right) \quad \text{if} \quad s = s_l^e\,, \tag{2.29}$$

$$[x_h^e]\,|_s = \left(x_h^e|_{s_u^e} - x_h^{e+1}|_{s_l^{e+1}}\right) \quad \text{if} \quad s = s_u^e\,, \tag{2.30}$$

$$[x_h^e]\,|_s = \left(x_h^{e-1}|_{s_u^{e-1}} - x_h^e|_{s_l^e}\right) \quad \text{if} \quad s = s_l^e\,. \tag{2.31}$$

The only modification compared to standard LDG methods is the inclusion of a second penalty term scaled by η_2 and proportional to the jump in velocity at the boundary. Although this introduces numerical damping in the formulation, it quickly minimises numerical fluctuations at the elemental boundaries without any noticeable loss of energy.

2.4 Boundary Conditions

The boundary conditions of the cable are weakly implemented through the fluxes of the LDG scheme. Instead of the internal fluxes in (2.26) and (2.27), specific boundary fluxes according to (2.32) and (2.33) are used.

$$\widehat{\mathbf{r}_h} = \mathbf{g}_\mathrm{D} \quad \text{on } \Gamma_\mathrm{D}\,, \qquad \widehat{\mathbf{r}_h} = \mathbf{r}_h^e \quad \text{on } \Gamma_\mathrm{N} \tag{2.32}$$

$$\widehat{\mathbf{T}_h} = \mathbf{T}_h^e + \frac{\eta_1}{h}\,(\mathbf{r}_h^e - \mathbf{g}_\mathrm{D}) \quad \text{on } \Gamma_\mathrm{D}\,, \qquad \widehat{\mathbf{T}_h} = \mathbf{g}_\mathrm{N} \quad \text{on } \Gamma_\mathrm{N} \tag{2.33}$$

Here $\mathbf{g}_\mathrm{D}$ and $\mathbf{g}_\mathrm{N}$ are the Dirichlet and Neumann boundary condition values at the cable end points.

2.5 Automated Program Interface

MooDy uses an Automated Program Interface (API) to communicate with external solvers, here exemplified by a solver for the hydrodynamic motion of the moored device. The hydrodynamic code acts as the *parent* software, and takes the leading role in the explicit API-loop shown in figure 2.1. The *parent* proceeds

in time by taking a time-step, the new mooring point positions and the new time are sent to MooDy, where they are used as a time dependent Dirichlet boundary condition; see eq. (2.32)-(2.33). MooDy then returns the mooring force at the new time, and this is in turn used as an input for the evaluation of the next time step of the *parent* solver. If the time step scheme of the *parent* is implicit, the loop will be iterated and MooDy will simply calculate the force for each trial value of the mooring point positions.

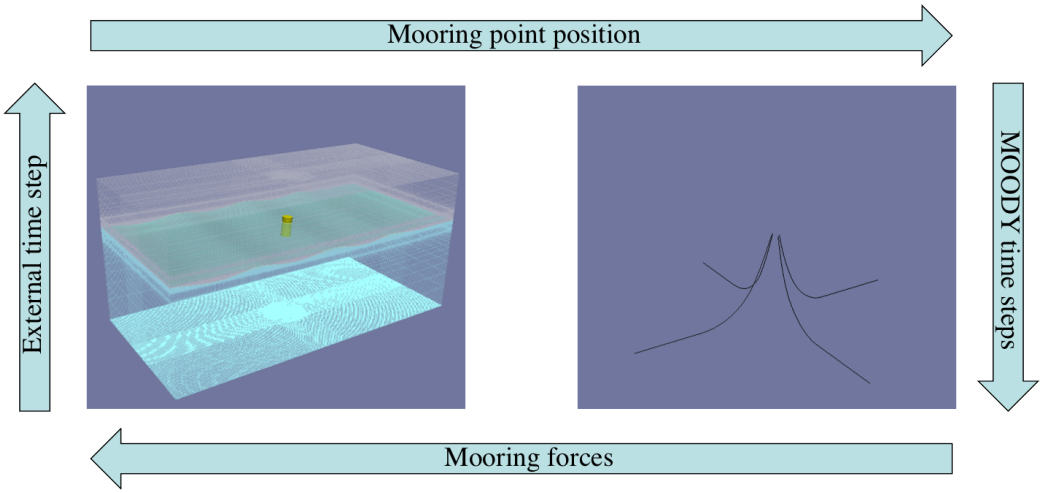

Figure 2.1: Schematic description of the API coupling procedure

2.5.1 Substepping methods

Due to the different time-step restrictions of the two solvers (where MooDy in most cases requires a smaller time step), a sub-stepping routine is required for the softwares to efficiently coexist. Thus, the boundary condition at the cable attachment point for all sub-steps must be interpolated between the known values sent to the API at the *parent* time steps. This can be done in several ways, depending of which assumptions that can be made about the external point motion. Here two methods are presented, linear and quadratic interpolation.

Let t_i, r_i, v_i, and a_i be the time, position,velocity and acceleration at time step index i, and let $\Delta_i = t_{i+1} - t_i$ symbolise the time step length. Thus, simple linear interpolation of the position boundary condition for $t \in [t_i, t_{i+1}]$ gives:

$$r(t) = \frac{t_{i+1} - t}{\Delta_i} r_i + \frac{t - t_i}{\Delta_i} r_{i+1}\,, \tag{2.34}$$

$$v(t) = \frac{r_{i+1} - r_i}{\Delta_i}\,, \tag{2.35}$$

$$a(t) = 0\,. \tag{2.36}$$

This requires a relatively smooth external motion (or a relatively small *parent* time step) as it introduces discrete directional changes at each *parent* time. The results presented in this thesis are from this approach.

A smoother solution is achieved using quadratic interpolation under the assumption that the velocity at the start of time step is the time-weighted average over the previous and present time-steps. This interpolates the motion for $t \in [t_i, t_{i+1}]$ as a quadratic polynomial:

$$v_i = \frac{r_{i+1} - r_i}{\Delta_{i-1}} \frac{\Delta_i}{\Delta_{i-1} + \Delta_i} + \frac{r_i - r_{i-1}}{\Delta_i} \frac{\Delta_{i-1}}{\Delta_{i-1} + \Delta_i}, \tag{2.37}$$

$$a_i = 2 \frac{r_{i+1} - r_i - v_1 \Delta_i}{\Delta_i^2}, \tag{2.38}$$

$$r(t) = r_i + v_i(t - t_i) + 0.5 a_i (t - t_i)^2, \tag{2.39}$$

$$v(t) = v_i + a_i(t - t_i). \tag{2.40}$$

3

Summary of papers

3.1 PAPER I

Mooring Cable Dynamics using a Discontinuous Galerkin Method describes the mathematical formulation and the FE discretisation of MooDy, see chapter 2. Further, Paper I presents three test cases to validate and verify the performance of the mooring code.

Case 1
A static verification study on the convergence of the discretisation for a hanging catenary shape.

Case 2
A dynamic convergence verification for a standing wave.

Case 3
A validation study where the end-point force is compared with experimental data.

The verification cases 1 and 2 show exponential convergence, with the dynamic test (case 2) degrading to sub-optimal convergence due to the choice of opposing fluxes. This is in good agreement with the theoretical predictions for high-order elements, see [18]. Figure 3.1 shows the L_2-norm error of case 1 as a function of increasing h and p resolution.

Case 3 is based on experiments presented in [22]. A circular motion of radius $r = 0.2\,\mathrm{m}$ was imposed on the end-point of a 33 m long chain, suspended in 3 m of water. The numerical prediction of the end-point force was compared with the experimental values, showing good agreement between them. Figure 3.2 shows the results from a 3.5 s period circular end-point motion.

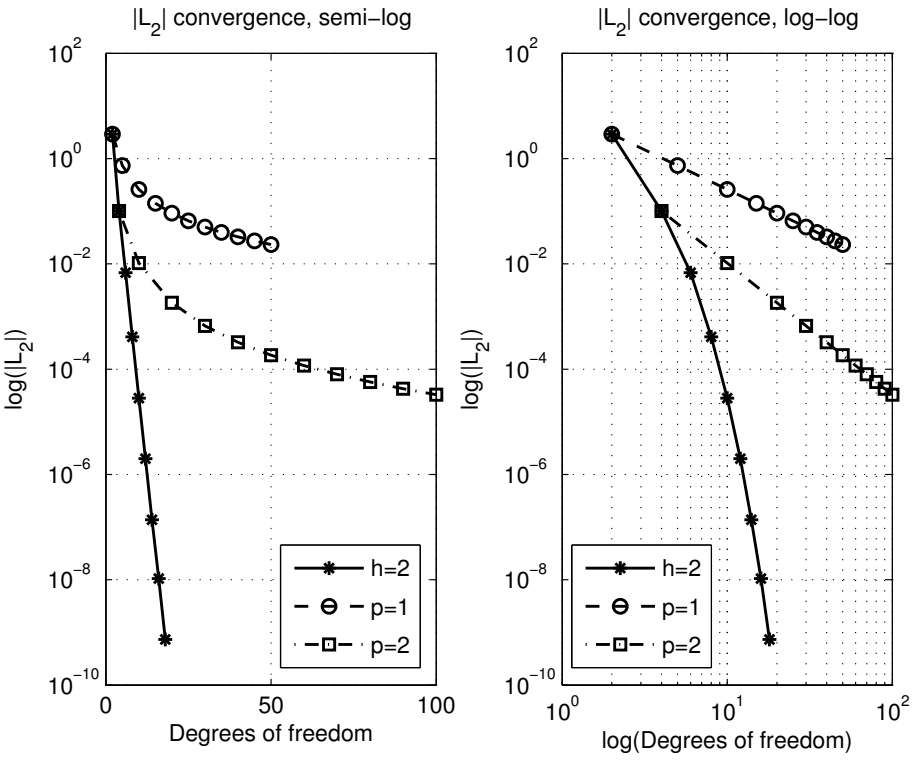

Figure 3.1: Convergence results from case 1, the static verification test of Paper I. Here p denotes polynomial order of the basis functions, and h is the number of elements. The number of degrees of freedom (x-axis) in the simulation is $h(p+1)$. $|L_2|$ represent the total error in position of the cable.

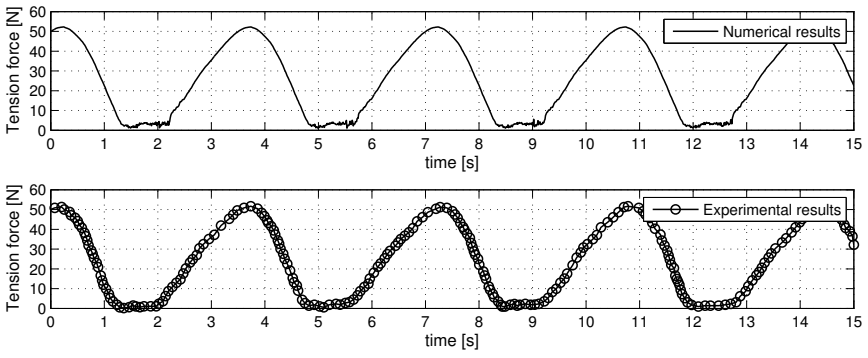

Figure 3.2: Comparison between numerical and experimental results of a laboratory chain. The end-point was forced to move in a $r = 0.2$m radius circle with a 3.5s period.

3.2 PAPER II

Experimental and Numerical Modelling of a Generic, Floating Wave Energy Converter describes model tests of a moored buoy in regular waves, and shows experimental results compared with numerical simulations. The numerical results are from MooDy simulations of a catenary mooring chain in 0.9 m water depth, coupled to a linear solver for rigid body motion in waves. The moored buoy was a standing cylinder with a total displacement of approximately 35 kg. Figure 3.3 shows the experimental schematics.

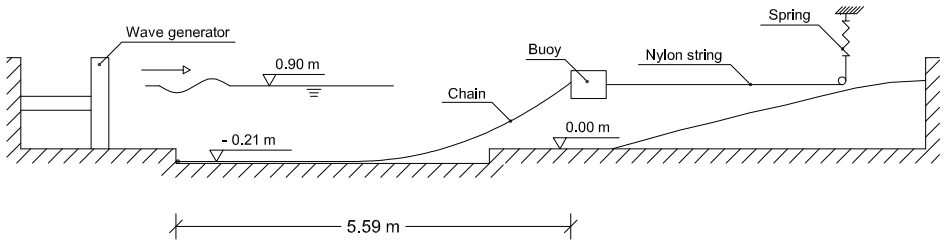

Figure 3.3: Schematic sketch of the experimental setup.

The main behaviour of the tension force are captured by the coupled model, however, the actual force magnitude needs more careful explanation. The lack of mean drift force in the simulation renders inaccurate motion results in surge, which lowered the simulated values of the tension force. As the load cell was not pressure compensated, the experimental force readings are also offset, and read around 0.7N too low. Thus, both the experimental and numerical results shown in figure 3.4 are lower than the true value.

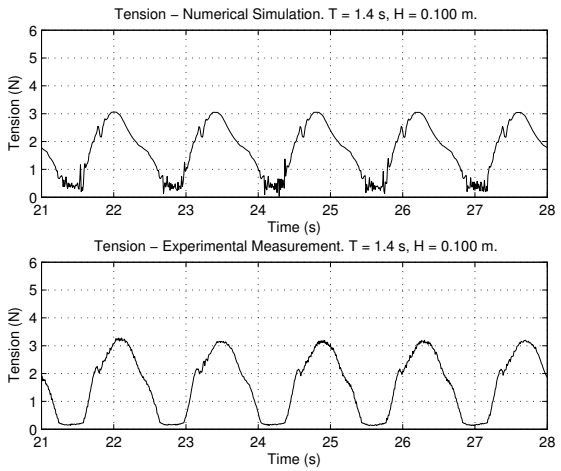

Figure 3.4: Comparison between numerical and experimental tension force at the cable end-point. The wave height was here 10 cm at a period time of 1.4 s.

3.3 PAPER III

CFD Simulations of a Moored Floating Wave Energy Converter presents preliminary results from CFD simulations of a moored, generic WEC in full scale. Simulations of a standing 100 tonne cylinder, moored with 4 catenary chains in regular waves are realised using an automated coupling between a two-phase VoF-solver of OpenFOAM [25] and MooDy. At each time step, the rigid body solver in OpenFOAM sends the present positions of all mooring attachment points, and MooDy computes the resulting restraining force on the motion. The coupling is based on a generic coupling allowing OpenFOAM to execute Matlab commands during simulations. This was realised by linking to the Matlab engine as described by the author in [27].

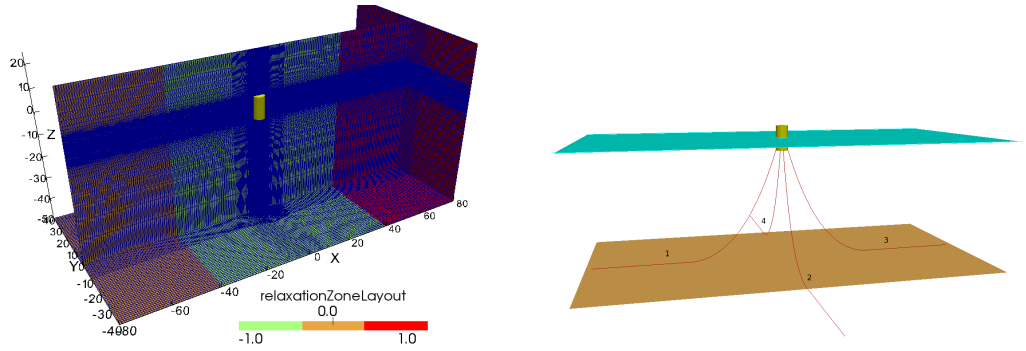

(a) Mesh layout (b) Initial geometry

Figure 3.5: (a) shows the relaxation zone layout and the computational grid, and (b) shows the initial geometry of the mooring system and the cylinder.

Results from the case study depicted in figure 3.5 show the general behaviour of the model in regular waves, and how the mooring affects the motion of the body. There is a clear dependence on wave height in the resonance region of the cylinder, where the Response Amplitude Operator (RAO) is significantly larger for a 1 m wave than for a 2 m wave. As the model includes many non-linearities that are disregarded in linear theory, the main reason for this change in RAO is not identified although numerical under-resolution of the body boundary-layer may be a contributing factor. Figure 3.6 shows the heave response of four different test cases. The left graph shows the difference between moored and unmoored device, as well as the effect of a Power Take Off (PTO) that dampens the motion of the body. Due to ground interaction, there are some high frequency oscillations in the force results, showing the importance of the ground model implementation for the resulting end-point tension force.

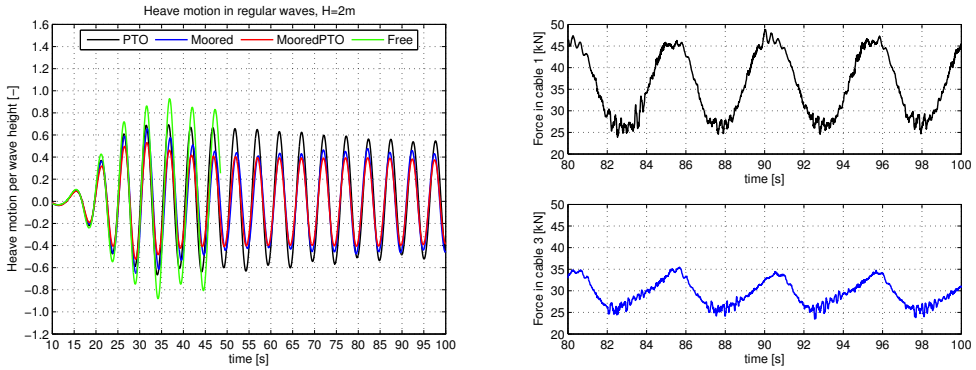

(a) Heave motion

(b) Tension force

Figure 3.6: Results from regular 2 m waves at a period time of 5 s. (a) Heave motion with and without mooring and PTO. The *Free* case experienced excessive drift after some time in the simulation. (b) Tension force in the seaward and the leeward mooring cables of the body for the *Moored* case.

4

Discussion

The focus of this thesis has been on the development of computational tools for mooring analysis and for hydrodynamic simulation of the motion of moored floating objects in waves. It has been separated into two parts: the development of MooDy as a FE tool for analysis of mooring cable dynamics (mainly Paper I); and the study of the coupled approach for computing the motion of moored floating objects (Paper II and III). MooDy and the coupled models are tools developed to analyse and quantify non-linear effects in floating WEC motion in waves. However, as the results presented here are not yet comprehensive enough to draw any final conclusions, the following discussion is focused on the benefits and drawbacks of the implementation and the chosen computational methods.

4.1 MOORING CABLE DYNAMICS

MooDy was presented as a tool for analysing shock-waves in mooring cables. It combines two features: high-order elements, and discontinuous elements. From paper I, the support of high-order basis functions promises a very high accuracy at a low computational cost, when the solution is smooth. For non-smooth solutions, high-order elements give rise to Gibbs-type oscillations. Such oscillations are to some extent relaxed by the Discontinuous Galerkin (DG) formulation that allows the solution to be discontinuous across element boundaries, but high-order elements are still ineffective around shocks. Thus, the optimal resolution is dependent on the appearance of the solution, where shocks are best captured by many low order elements while convergence of smooth solutions is more efficiently achieved through few elements of high order. Implementing an adaptive scheme for the h (number of elements) and p (polynomial order) discretisation - see e.g. [11] - is a well known solution to this, giving the solver the best parts of both features. The required resolution in h and p is set through an error estimator checking the smoothness of the solution. The development of the adaptive scheme

is ongoing.

The computational speed of MooDy is now limited by the software environment, Matlab. Much speed would be gained by moving over to a faster environment (such as C++ or Fortran), and only then can the efficiency of the formulation be investigated and compared with commercial codes.

The results show how the ground interaction influences the mooring response of slack mooring systems. There are two main reasons for this, the first being the discontinuous nature of the normal force close to the TDP (Touch Down Point). As was shown in [29] this can lead to shock-wave propagation when the TDP speed exceeds the transverse wave speed of the cable. Secondly, the level of damping in the system is to a large extent dependent on the ground model. In standard FE models (with continuous and linear elements), there is a high level of numerical damping that diffuses steep fluctuations in the tension force. In MooDy, the numerical damping is small, and these fluctuations must be damped through the reaction forces from drag, internal (axial) damping and ground interaction. The axial damping in the case of chains is very small and therefore the choice of friction model for tangential friction on the ground becomes very important, especially at model scale where the tension variations are small.

In order to properly validate a code for mooring dynamics against experimental results, the mooring force data needs to be of high quality with known and well-determined wave and current measurements, preferably synchronised with highly resolved displacement measurements. This is clearly difficult to achieve in sea-trials, and therefore large-scale experimental tests are needed for further development of mooring codes. However, full-scale sea-trial data must be used for the final benchmarking of the sophistication level needed in mooring cable analysis of WECs.

4.2 HYDRODYNAMIC SIMULATIONS

Today, there are several types of hydrodynamic models, with varying complexity and computational cost. Hence a trade-off between accuracy and computational speed must be made. It is therefore important to choose models that best fit the purpose of the calculation. Simplified and fast numerical models are widely used to estimate the annual power-production of a device, but the accuracy of these methods is questionable. CFD cannot make such a prediction due to the large computational times, but it can provide a way to quantify the non-linear effects on the WEC motion, and thereby benchmark the limitations of simpler hydrodynamic models.

CFD was here presented as a complete tool for handling the large non-linear effects of a floating WEC, both in resonant motion and under storm conditions. A computational model for full-scale evaluation of the performance of WECs can prove a powerful tool for wave-power developers, especially in the late stages of commercialisation. Here again the lack of good, large-scale data is unfortu-

nate. With well-determined waves from large-scale lab tests with good measuring equipment, the model could be validated with a decreased uncertainty regarding scale effects and the complexity of the three-dimensional ocean waves.

Even with a fully validated model, the computational cost for CFD simulations will be large. However, the computational cost must be put in perspective to the financial cost of sea-trials, which is substantial. CFD tools are well-used and trusted in other marine applications [19], and there is seemingly no reason why this could not be the case in the future development of the wave-power industry.

REFERENCES

[1] O.M. Aamo and T.I. Fossen. Finite element modelling of mooring lines. *Math. Comp. Sim.*, 53:415–422, 2000.

[2] E.B. Agamloh, A.K. Wallace, and A. von Jouanne. Application of fluid-structure interaction of an ocean wave energy extraction device. *Renewable Energy*, 33(4):748–757, 2008.

[3] S. Aliabadi, J. Abedi, and B. Zellars. Parallel finite element simulation of mooring forces on floating objects. *Int. J. Numer. Meth. Fluids*, 41:809–822, 2003. DOI:10.1002/fld.459.

[4] A. Babarit, J. Hals, M.J. Muliawan, A. Kurniawan, T. Moan, and J. Krokstad. Numerical benchmarking study of a selection of wave energy converters. *Renewable Energy*, 41:44–63, 2012.

[5] M.A. Bhinder, A. Babarit, L. Gentaz, and P. Ferrant. Assessment of viscous damping via 3d-cfd modelling of a floating wave energy device. In *Proc. EWTEC 2011*, Southampton, United Kingdom, 2011.

[6] D.T. Brown and S. Mavrakos. Comparative study on mooring line dynamic loading. *Marine Structures*, 12:131–151, 1999.

[7] B. Cockburn and C.-W. Shu. Runge-kutta discontinuous galerkin methods for convection-dominated problems. *J. Sci. Comp.*, 16:173–261, 2001.

[8] W.E. Cummins. The impulse response function and ship motions. *Schiffstechnik*, 9:101–109, 1962.

[9] Det Norske Veritas. *Position Mooring*, 2010. Offshore standard DNV-OS-301.

[10] Det Norske Veritas. *Design of Floating Wind Turbine Structures*, June 2013. Offshore standard DNV-OS-J103.

[11] C. Eskilsson. An hp-adaptive discontinuous galerkin method for shallow water flows. *Int. J. Numer. Meth. Fluids*, 67:1605–1623, 2011.

[12] J. Fitzgerald. *Position Mooring of Wave Energy Converters*. PhD thesis, Chalmers University of Technology, 2009.

[13] J. Fitzgerald and L. Bergdahl. Including moorings in the assessment of a generic offshore wave energy converter: a frequency domain approach. *Marine Structures*, 21:23–46, 2008.

[14] J. Fitzgerald and B Bolund. Technology readiness for wave eenergy projects; esb and vattenfall classification system. In *Proc. ICOE 2012*, Dublin, Ireland, 2012.

[15] J.I. Gobat and M.A. Grosenbaugh. Dynamics in the trouchdown region of catenary moorings. In *Proc. ISOPE 2001*, Stavanger, Norway, 2001.

[16] L. Johanning, G. Smith, and J. Wolfram. Measurements of static and dynamic mooring line damping and their importance for floating wec devices. *Ocean Engng.*, 34:1918–1934, 2007.

[17] M. Johansson. Transient motions of large floating structures. Technical Report Report Series A:14, Chalmers University of Technology, 1986.

[18] G. E. Karniadakis and S. Sherwin. *Spectral/hp Element Methods for CFD*. Oxford University Press, New York, Oxford, 2nd edition edition, 2003.

[19] L. Larsson, F. Stern, and M. Visonneau. *Numerical Ship Hydrodynamics*. Springer, New York, 2010.

[20] Y. Li and M. Lin. Regular and irregular wave impacts on floating body. *Ocean Eng.*, 42:93–101, 2012.

[21] J. Lindahl. Implicit numerisk lösning av rörelseekvationerna för en förankringskabel. Technical Report Report Series A:11, Chalmers University of Technology, 1984.

[22] J. Lindahl. Modellförsök med en förankringskabel. Technical Report Report Series A:12, Chalmers University of Technology, 1985.

[23] N. Mitchell and A. Ramzan. Design aspects of offshore mooring systems. *The Naval Architect*, 1986.

[24] A. Montano, M. Reselli, and R. Sacco. Numerical simulation of tethered buoy dynamics using mixed finite elements. *Comp. Meth. Appl. Mech. Engng*, 196:4117–4129, 2007.

[25] OpenCFD Ltd (2014). *OpenFOAM homepage. [Online]*. Available http://www.openfoam.org.

[26] Orcina Inc. *OrcaFlex manual – version 9.5a*, 2012.

[27] J. Palm. *Connecting OpenFOAM with MATLAB. [Online]*. Chalmers University of Technology. Available http://www.tfd.chalmers.se/ hani/kurser/OS_CFD_2012/.

[28] K. Spak, G. Agnes, and D. Inman. Cable modeling and internal damping developments. *Applied Mechanics Reviews, ASME*, 65(1), 2013.

[29] M.S. Triantafyllou, A. Bliek, and H. Shin. Dynamic analysis as a tool for open-sea mooring system design. *SNAME Transactions*, 93:302–324, 1985.

[30] WAMIT Inc. *WAMIT User Manual (version6.4)*.

[31] J. Weber, R. Costello, and J. Ringwood. Wec technology readiness and performance matrix - findeing the best research technology development trajectory. In *Proc. ICOE 2012*, Dublin, Ireland, 2012.

[32] Y. Yu and Y. Li. Preliminary results of a rans simulation for a floating point absorber wave energy system under extreme wave conditions. In *Proc. OMAE 2011*, 2011.

[33] Z. Yu and J. Falnes. State-space modelling of a vertival cylinder in heave. *Applied Ocean Research*, 17:265–275, 1995.